3. Rakic, P. & Sidman, R. L. *J. comp. Neurol.* **152,** 103–132 (1973).
4. Rakic, P. & Sidman, R. L. *J. comp. Neurol.* **152,** 133–162 (1973).
5. Sotelo, C. & Changeux, J.-P. *Brain Res.* **67,** 519–526 (1974).
6. Moonen, G., Grau-Wagemans, M. P. & Selak, I. *Nature* **298,** 753–755 (1982).
7. Rathjen, F. G. & Schachner, M. *EMBO J.* (in the press).
8. Miale, J. L. & Sidman, R. L. *Expl Neurol.* **4,** 277–296 (1961).
9. Goridis, C., Joher, J. A., Hirsch, M. & Schachner, M. *J. Neurochem.* **31,** 531–539 (1978).
10. Rohrer, H. & Schachner, M. *Neurochemistry* **35,** 792–803 (1980).
11. Jorgensen, O. S., Delouvee, A., Thiery, J.-P. & Edelmann, G. M. *FEBS Lett.* **111,** 39–42 (1980).
12. Hirn, M., Pierres, M., Deagostini-Bazin, H., Hirsch, M. & Goridis, C. *Brain Res.* **214,** 433–439 (1981).
13. Brackenbury, R., Thiery, M.-P., Rutishauser, U. & Edelman, G. M. *J. biol. Chem.* **252,** 6835–6840 (1977).
14. Hoffman, S. *et al. J. biol. Chem.* **257,** 7720–7729 (1982).
15. Lemmon, V., Staros, E. B., Perry, H. E. & Gottlieb, D. I. *Devl Brain Res.* **3,** 349–360 (1982).
16. Schnitzer, J. & Schachner, M. *J. Immun.* **1,** 457–470 (1981).
17. Altman, J. *J. comp. Neurol.* **163,** 427–448 (1975).
18. Caviness, V. S. & Rakic, P. *A. Rev. Neurosci.* **1,** 297–326 (1978).
19. Fischer, G. *Neurosci. Lett.* **28,** 325–329 (1982).
20. Goridis, C., Martin, J. & Schachner, M. *Brain Res. Bull.* **3,** 45–52 (1978).
21. Willinger, M. & Schachner, M. *Devl Biol.* **74,** 101–117 (1980).
22. Fujita, S. *J. Cell Biol.* **32,** 277–287 (1967).

Motility and mechanosensitivity of macrocilia in the ctenophore *Beroë*

Sidney L. Tamm

Boston University Marine Program, Marine Biological Laboratory, Woods Hole, Massachusetts 02543, USA

Mechanical activation of the microtubule sliding mechanism in cilia and flagella[1–3] by local passive bending has been postulated to be essential for the initiation and propagation of bending waves along the axoneme[4,5]. In addition, responsiveness of cilia to hydrodynamic forces imposed externally by their neighbours is thought to be responsible for metachronal coordination of ciliary activity[6–10], as well as for synchronal beating of component cilia within compound ciliary organelles[11,12]. Direct tests of the mechanosensitivity of motile cilia are limited, but generally support these views[7,10,11,13–18]. It remains problematical, however, whether mechanical interaction between cilia operates continuously during both the effective and recovery phases of the asymmetrical beat cycle. Moreover, the directional sensitivity and temporal responsiveness of motile cilia to mechanical stimuli have been explored in only a few cases[7,10.14]. Finally, the continuous nature of the ciliary beat cycle has hindered investigation of the 'switch point hypothesis' in which doublet sliding is assumed to be activated sequentially on the two halves of the axoneme to produce bends in opposite directions[19]. Here we report that macrocilia[20] on the ctenophore *Beroë* beat discontinuously with separate effective and recovery strokes, resulting in 'split-cycle' waves of metachronal coordination. This new pattern of ciliary beating is used to investigate the motile responses of cilia to controlled mechanical stimuli during each phase of the beat cycle.

Macrocilia are thick cylindrical organelles found in a dense band around the inner margin of the lips of beroid ctenophores. A single macrocilium is 35–40 μm long and ~5 μm in diameter, and consists of ~2,500 ciliary axonemes cross-linked to one another and surrounded by a common membrane[20]. Macrocilia beat in a planar ciliary type of pattern with the effective (power) stroke directed away from the mouth. Continuous activity is rarely observed, but when this does occur the cilia beat at 3–5 Hz, with antiplectic metachronal waves sweeping in irregular patterns towards the mouth at 250–300 μm s^{-1}.

More typically, macrocilia exhibit an intermittent type of activity termed split-cycle coordination (Fig. 1). At any instant, most of the macrocilia lie at rest at an angle of about 30° to the lip surface with their distal ends overlapping and pointing away from the mouth in the position reached at the end of the effective stroke. Split cycle waves begin at irregular intervals along the aboral edge of the band when a few macrocilia initiate recovery stroke bends towards the mouth. These distally propagated flexions impinge directly on overlying cilia in the oral direction, lifting them upward and stimulating them into similar activity, which in turn excites their neighbours further orally. A wave of recovery strokes thus travels towards the mouth in a distinct tract, usually 10–20 cilia wide (Fig. 1*a–c*, *a′–c′*). The recovery wavefront, which represents the packed distal ends of the unrolling cilia, advances slowly at a speed of 50 ± 6.5 μm s^{-1} ($n = 12$). The recovery stroke wave usually broadens as it spreads orally, giving the tract a fan-shaped appearance. The macrocilia do not perform an effective stroke immediately, but remain frozen in a sigmoid posture at the end of the recovery stroke for a short time interval. Passage of a recovery wave through a field of resting macrocilia thus leaves a sharply delineated swath of cilia pointing in the opposite, upstream direction.

After a brief time delay, each macrocilium performs an effective stroke and completes the beat cycle before returning to rest. The time interval between the end of the recovery stroke and the onset of the power stroke ranges from 11 ± 1.5 s to 13 ± 1.6 s ($n = 28$). Although the first cilia to perform an effective stroke are near the aboral end of the tract, a wave of power strokes does not proceed uniformly towards the mouth. Instead, slight variations in the latency between the recovery and effective strokes cause the power stroke to be initiated independently at various locations along the tract, but generally in an aboral–oral sequence. If a macrocilium which makes an effective stroke hits recovery-pointing cilia downstream before they beat spontaneously, these cilia respond by an active power stroke. A wave of effective strokes, usually only a few macrocilia wide, then propagates in an aboral direction for a short distance, ending at cilia further downstream which have already performed their effective stroke (Fig. 1*d*, *e*, *d′*, *e′*). The velocity of the effective stroke waves is 175 ± 56 μm s^{-1} ($n = 17$), or about four times faster than the recovery waves, reflecting the greater angular velocity and closer mechanical coupling between cilia in the effective stroke. After completing the effective stroke, all the macrocilia once again lie at rest pointing away from the mouth, erasing all signs of the original recovery stroke tract (Fig. 1*f*, *f′*). The band of macrocilia is usually covered with many such tracts of split-cycle waves, each acting independently of one another. That this novel pattern of ciliary coordination is not an artefact of excised lip preparations is shown by the presence of split-cycle waves in macrocilia of intact whole baby *Beroë* (1–2 mm long) viewed by Nomarski microscopy.

To investigate the mechanosensitivity of macrocilia further, controlled mechanical stimuli were applied to the cilia at different stages in the beat cycle using fine glass needles operated by a micromanipulator. When resting macrocilia are lifted away from the body surface by a micro-needle pushed in the oral direction, a wave of recovery strokes is initiated which propagates towards the mouth at a velocity of 55 ± 11 μm s^{-1} ($n = 7$) (Fig. 2), similar to the speed of naturally occurring recovery waves. The cilia remain in a sigmoid flexion at the end of the recovery stroke for a short time, and then perform effective strokes as described above. Movement of the micro-needle in the opposite (aboral) direction across the tips of resting macrocilia does not stimulate recovery strokes. Pressing resting macrocilia down against the epithelial surface with a needle stopped the propagation of recovery waves which had begun spontaneously on the aboral side of the needle, further showing that recovery stroke waves are coordinated by viscomechanical coupling between the cilia.

When the tip of a macrocilium temporarily arrested at the end of the recovery stroke is deflected 5–10 μm in the aboral direction by a micro-needle, a single effective stroke may be induced (Fig. 3). The time course of responsiveness to mechanical stimuli was investigated by applying repetitive displacements in the aboral direction to the distal ends of small groups of recovery-pointing cilia, starting 3–5 s after the end of the recovery stroke. In one case, mechanical stimuli delivered at 2-s intervals did not elicit effective strokes until 9 s following the preceding recovery stroke. In another example, a micro-

0028–0836/83/390430—03$01.00

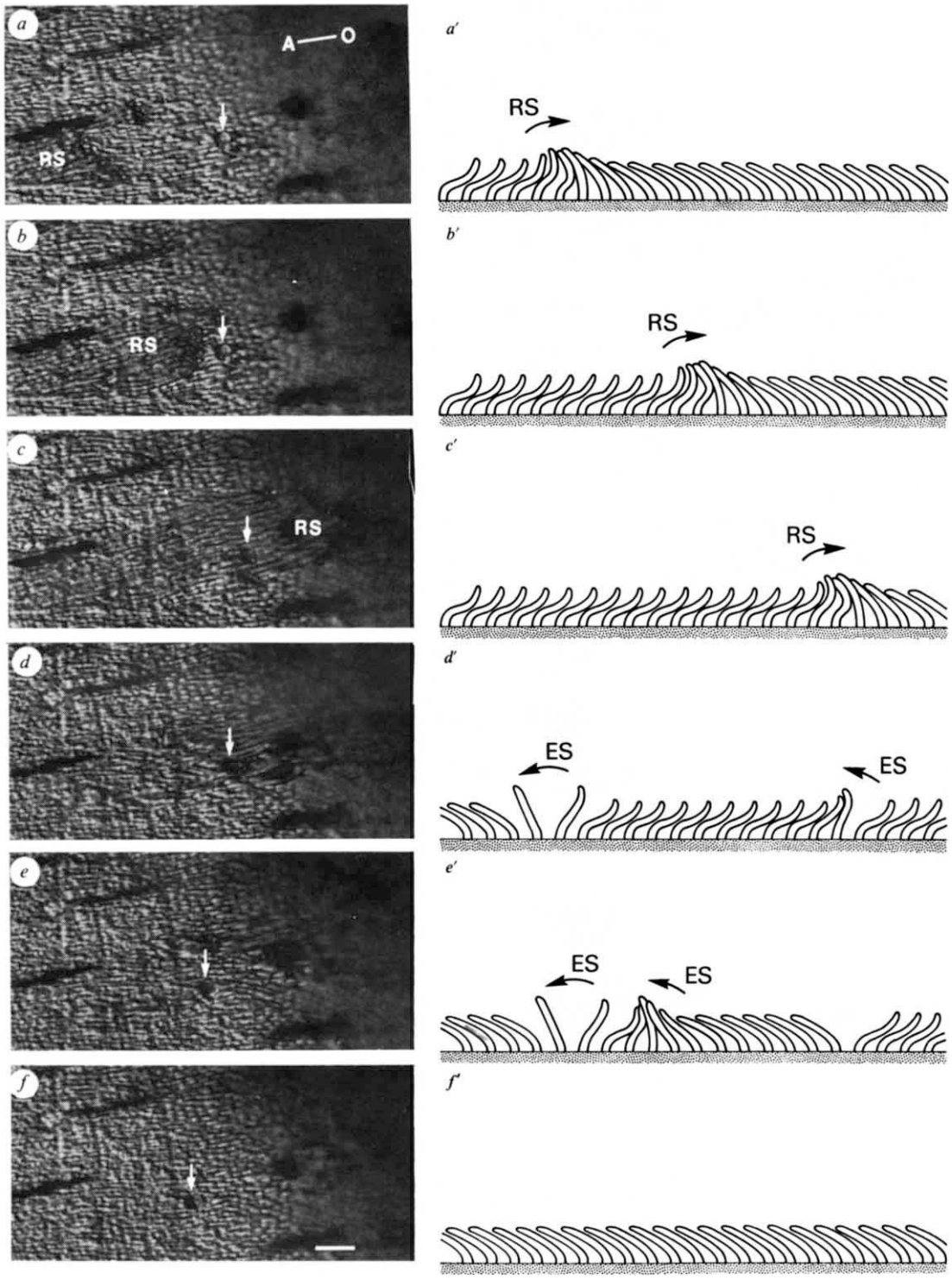

Fig. 1 Face view of field of macrocilia showing sequence of split cycle coordination (Zeiss Nomarski optics, prints from cine film at 2.0-, 3.4-, 8.2-, 0.8- and 5.5-s intervals). *a′–f′*, Diagrams of corresponding stages viewed in profile. *a–c* and *a′–c′*, Recovery stroke wavefront (RS) advancing in an aboral–oral direction (A–O axis), from reader's left to right. Resting macrocilia lie at the end of the effective stroke pointing away from the mouth, and are lifted away from the surface by recovery bends of their neighbours aborally, thereby stimulating a wave of recovery strokes which propagates in the oral direction (RS arrows, *a′–c′*). Macrocilia behind the wavefront remain arrested in a sigmoid flexion at the end of the recovery stroke, leaving a swath of recovery-pointing cilia surrounded by effective-pointing cilia (*a–c*). A particle (arrows, *a–c*) is displaced a short distance in the oral direction by the passing wavefront. *d*, *d′*, Initiation of the effective stroke after variable time delays at different places along the RS tract, but generally in an aboral–oral sequence. *d*, Most macrocilia on the left side of the tract have completed a power stroke, but those to the right of the particle (arrow) are still doing so. *d′*, Macrocilia on the left are performing an effective stroke (ES arrow) in an aboral–oral sequence; macrocilium on right (ES arrow) initiates an effective stroke prematurely. *e*, Most macrocilia have now performed a power stroke, pushing the particle (arrow) further to the left. *e′*, The premature power stroke by the macrocilium on the right has triggered a wave of effective strokes in macrocilia aboral to it, but this ES wave travels only a short distance to the left before meeting cilia downstream which have already performed a power stroke. *f*, *f′*, All macrocilia in the tract have completed an effective stroke and lie at rest pointing away from the mouth, erasing all signs of the original recovery stroke wave. The particle (arrow, *f*) has undergone a net displacement to the left (compare with position in *a*) in the direction of the power stroke. Lips of *Beroë cucumis* were excised and mounted in a slide chamber filled with seawater or $MgCl_2$–seawater (1:1) to relax muscles. Scale bar (*a–f*), 50 μm.

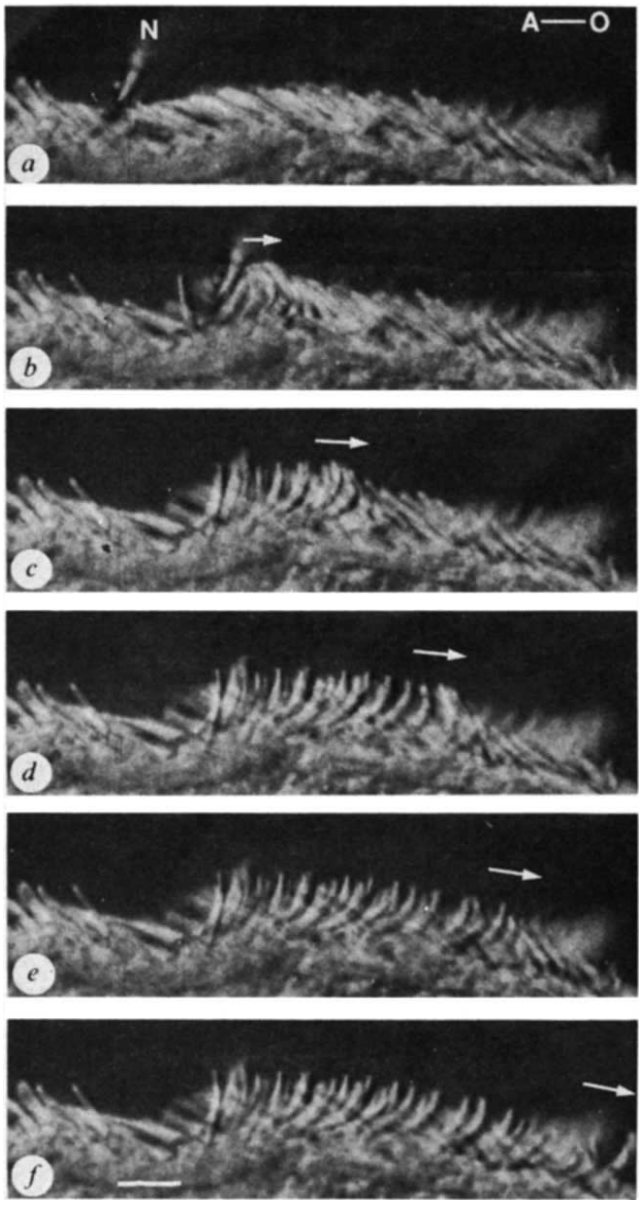

Fig. 2 Mechanical stimulation of a recovery stroke wave in resting macrocilia. Macrocilia are viewed in profile on a thin slice of lip by Nomarski optics. *a*, Before stimulation with a glass needle (N), macrocilia lie over one another pointing in the aboral direction (A–O, aboral–oral axis). *b*, Displacement of several macrocilia to the right (arrow) triggers recovery bends in the oral direction. *c–f*, A wave of recovery strokes propagates towards the mouth (arrows) as cilia in the oral direction are successively pushed upward by their neighbours aborally and stimulated to perform a recovery stroke. Macrocilia remain arrested in a sigmoid posture at the end of the recovery stroke for a brief time before initiating an effective stroke (not shown). Prints from cine film at 0.63-s intervals. Scale bar, 25 μm.

needle driven by a piezoelectric probe[21] was used to deliver 10-μm displacements (0.08 s excursion time) at 1-s intervals to the tips of recovery-pointing macrocilia. No response occurred for 6 s following the recovery stroke; a stimulus at 7 s induced some cilia to perform a power stroke, and the next stimulus at 8 s triggered a few more cilia to do so. The remaining cilia were not activated to perform an effective stroke until 12 s after their recovery stroke.

Therefore, macrocilia arrested at the end of their recovery stroke show a variable period of insensitivity to mechanical stimuli before responding by an active power stroke. This refractory period ends before the cilia perform an effective stroke spontaneously. The motile response of other cilia to mechanical

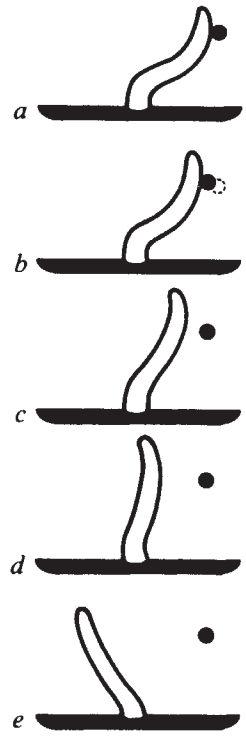

Fig. 3 Mechanical stimulation of the effective stroke in a single recovery-pointing macrocilium. *a*, Micro-needle (black cross-section) is positioned behind the distal end of a macrocilium arrested for the preceding 12.6 s at the end of the recovery stroke (after the refractory period to mechanical stimuli has ended). *b*, The tip of the macrocilium is deflected 5–6 μm in the aboral direction (to reader's left) by the micro-needle. *c–e*, Initiation of a power stroke in the aboral direction. Tracings from cine film at 0.08-s intervals.

stimulation, excluding arrest responses[15], is usually a complete beat cycle[7,10,11,14,17]. The effectiveness of the stimulus is a function of its direction in some cases[10,14], but not apparently in others[17]. In contrast, the immediate response of macrocilia to mechanical stimulation is either an effective stroke or a recovery stroke, but not both. The direction of the active bending response of macrocilia corresponds to the direction of the stimulus. As bending in opposite directions is thought to result from activation of doublet sliding alternately in two halves of the axoneme[19,22], our findings indicate that either set of microtubules can be activated independently by mechanical stimuli applied in the direction of force generation.

A unique feature of the beat cycle of macrocilia is the existence of two different arrest positions, one at the end of the effective stroke and the other at the end of the recovery stroke. The resting phase at the end of the effective stroke is of indeterminate duration, lasting until mechanical stimuli trigger a recovery stroke. The pause at the end of the recovery stroke, on the other hand, has a rather constant period which ends spontaneously without external triggering, indicating an intrinsic timing device for activating sliding at the start of the effective stroke. This timing mechanism shows a refractory period during which the mechanosensitivity of the motile elements is reduced or lost. These results support the presence of two distinct switching mechanisms for activation of doublet sliding on opposite sides of the axoneme during a single beat cycle[19,22] and provide an advantageous system for experimental dissection of the control of microtubule sliding in cilia.

In split-cycle coordination, the recovery stroke waves and effective stroke waves travel in opposite directions, but in the same direction as their respective bending movements (Fig. 1). This provides a clear demonstration of the mechanical coordination of ciliary movement[6–12]. In addition, there observations show that mechanical coupling between responsive cilia can

occur during both the effective and recovery strokes, indicating that metachronism results from continuous mechanical interaction throughout the beat cycle[6,23].

Intermittent ciliary activity with resting phases following the end of each effective stroke (but with a continuous beat cycle) is also observed in rabbit tracheal and frog palate cilia, and seems to be an adaptation for mucus and particle transport[24]. The compounding of several thousand axonemes into a single macrocilium[20] would be expected to increase the stiffness and active bending moment of the organelle, allowing *Beroë* to engulf prey larger than itself, or to bite off pieces[10,25]. The single membrane surrounding each macrocilium, together with the extensive cross-linking of adjacent axonemes, may serve to prevent the organelle from fraying apart during the mechanical stresses associated with prey ingestion.

This work was supported by the NIH (grant GM 27903).

Received 24 May; accepted 27 July 1983.

1. Satir, P. *J. Cell Biol.* **26,** 805–834 (1965).
2. Satir, P. *J. Cell Biol.* **39,** 77–94 (1968).
3. Summers, K. E. & Gibbons, I. R. *Proc. natn. Acad. Sci. U.S.A.* **68,** 3092–3096 (1971).
4. Machin, K. E. *J. exp. Biol.* **35,** 796–806 (1958).
5. Brokaw, C. J. *Nature* **209,** 161–163 (1966).
6. Machemer, H. in *Cilia and Flagella* (ed. Sleigh, M. A.) 199–286 (Academic, London, 1974).
7. Murakami, A. *J. Fac. Sci. Univ. Tokyo IV* **10,** 23–35 (1963).
8. Tamm, S. L. *J. exp. Biol.* **59,** 231–245 (1973).
9. Sleigh, M. A. in *Cilia and Flagella* (ed. Sleigh, M. A.) 287–304 (Academic, London, 1974).
10. Tamm, S. L. in *Electrical Conduction and Behaviour in 'Simple' Invertebrates* (ed. Shelton, G. A. B.) 266–358 (Oxford University Press, 1982).
11. Tsuchiya, T. *Annotnes zool. jap.* **42,** 113–125 (1969).
12. Tamm, S. L. *Biol. Bull.* **159,** 446 (1980).
13. Kinosita, H. & Kamada, T. *Jap. J. Zool.* **8,** 291–310 (1939).
14. Thurm, U. *Symp. zool. Soc. Lond.* **23,** 199–216 (1968).
15. Murakami, A. & Machemer, H. *J. comp. Physiol.* **145,** 351–362 (1982).
16. Okuno, M. & Hiramoto, Y. *J. exp. Biol.* **65,** 401–413 (1976).
17. Sleigh, M. A. & Jarman, M. *J. mechanochem. Cell Motility* **2,** 61–68 (1973).
18. Baba, S. *Nature* **282,** 717–720 (1979).
19. Wais-Steider, J. & Satir, P. *J. supramolec. Struct.* **11,** 339–347 (1979).
20. Horridge, G. A. *Proc. R. Soc.* B**162,** 351–364 (1965).
21. Corey, D. P. & Hudspeth, A. J. *J. Neurosci. Meth.* **3,** 183–202 (1980).
22. Sugino, K. & Naitoh, Y. *Nature* **295,** 609–611 (1982).
23. Gray, J. *Proc. R. Soc.* B**107,** 313–332 (1930).
24. Sanderson, M. J. & Sleigh, M. A. *J. Cell Sci.* **47,** 331–347 (1981).
25. Swanberg, N. *Mar. Biol.* **24,** 69–76 (1974).

Correction of cell–cell communication defect by introduction of a protein kinase into mutant cells

Erik C. Wiener & Werner R. Loewenstein

Department of Physiology and Biophysics, University of Miami School of Medicine, PO Box 016430, Miami, Florida 33101, USA

The cell-to-cell permeability of the junctions of various cultured mammalian cell types depends on the concentration of intracellular cyclic AMP ($[cAMP]_i$). The permeability rises when the cells are supplied with exogenous cyclic AMP or when their cyclic AMP synthesis is stimulated with choleragen or hormones; it falls when $[cAMP]_i$ is lowered by application of serum or due to increase in cell density[1–5]. The rise and fall in permeability take several hours to develop (the rise is protein synthesis-dependent) and they occur concurrently with the rise and fall in the number of intramembrane particles of the gap junctions[2–4], which probably embody the cell-to-cell channels. Is this permeability regulation mediated by phosphorylating protein kinase? In many eukaryotes, the cyclic AMP receptor is a protein kinase[6–8] consisting of a pair of regulatory subunits and a pair of catalytic subunits. The latter dissociate from the holoenzyme as the cyclic AMP binds to the regulatory subunits and, in this dissociated form, catalyse the phosphorylation of the target[9]. The regulatory subunit occurs in two isoenzyme forms, I and II. The catalytic subunit seems invariant[9]; subunits from different isoenzymes can substitute for each other[10,11]. We show here that a mutant cell lacking the isoenzyme I is deficient in permeable junctions, and that this junctional defect is corrected when the mutant is supplied with exogenous catalytic subunit.

Chinese hamster ovary cells (wild-type clone 10001, mutant 10260 (I^-) and mutant 10215 (II^-), isolated in single-step selection[12], were given by Dr M. Gottesman. Mutant I^- has no protein kinase type I and has little of type II; mutant II^- has no protein kinase II and has type I (but this type I has a reduced cyclic AMP sensitivity[12] and the cell's endogenous cyclic AMP concentration is higher than in the wild cell). All three types of cells attached and spread on the culture dishes, establishing close contacts as seen by phase contrast microscopy. Junctional permeability was probed in single-layer cell cultures with carboxyfluorescein (molecular weight (MW) 376) and with glutamic acid labelled with lissamine rhodamine B (LRB-Glu, MW 688). We microinjected these fluorescent tracers into the cells and determined for each individually injected cell the incidence of permeable first-order interfaces, that is, the proportion of fluorescent cells among the cells contiguous to the injected one (Fig. 1). This incidence is a convenient index of changes in junctional permeability, and a particularly sensitive one when the probing molecule is close to detection threshold for junction permeation[4,5]. All comparisons were done at equal cell densities. For statistical analysis of differences we used the nonparametric Mann–Whitney U method.

Figure 2 gives the mean incidences of permeable interfaces in the three cell types for various density conditions. Mutant I^- had a significantly smaller incidence than the wild-type cell in all conditions ($P < 0.0005$). The difference between the incidences was most striking with the LRB-Glu probe, as this larger and more negatively charged molecule was close to the detection threshold of junction-permeation in mutant I^- (Fig. 2*c*, *d*; see also the example in Fig. 1). But even the probings with carboxyfluorescein, well above detection threshold, showed a clear difference ($P < 0.0005$) (Fig. 2*a*, *b*).

The junctional deficiency and its relation to the enzyme mutation is further demonstrated by clonal analysis of revertants. The I^- mutation was generally stable[12]. However, after growing for several months, a few cultures slowly developed higher base levels of junctional permeability; they seemed to be reverting

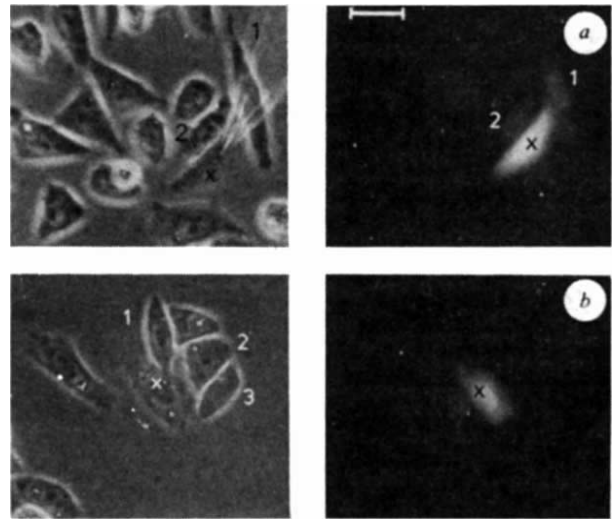

Fig. 1 Junctional probings with LRB-Glu in wild-type (*a*) and mutant I^- cultures (*b*). This probe is close to the detection threshold for junction permeation and therefore is a sensitive indicator of changes in junctional permeability. The injected cell in each cluster is marked by ×; the cells contiguous to it are numbered. Left, phase contrast (the injection micropipette is seen in the top part of the cell); right, fluorescence darkfield. Scale bar, 40 μM. The cells were grown and probed in HAM's F-12 medium with 10% fetal calf serum in plastic dishes (Falcon). They were fed three times weekly, with the last feeding 18 h before experiments, and passaged just before confluency. The last passage was at least 18 h before experiments. For preparation and purification of LRB-Glu, see ref. 20; for steric limits of the cell–cell channel, see ref. 21.

0028-0836/83/390433—03$01.00